

Analysis of the influence of the conductivity of bricks, type of bricks and size of the hollows on the values of the electric field intensity

Abstract. The aim of the publication is to analyse the influence of brick walls used in single-family housing on the values of the electric field intensity. Three types of bricks from which the wall was made were considered (solid brick, brick with 18 hollows and brick with 30 hollows). The analysis also took into account the impact of the size of the hollows on the field values and the variability of the conductivity of the brick. The results were compared for the arrangement with an asymmetric arrangement of bricks with a symmetrical arrangement, which may correspond to walls made of hollow bricks. The analysis concerned the frequency used in wireless communication (Wi-Fi), i.e. $f=2.4$ GHz. The influence of the size of the structural clay tile and the conductivity of bricks on the electric field values is discussed. A method based on Maxwell's equations (Finite Difference Time Domain Method), was used for the analysis.

Streszczenie. Celem publikacji jest analiza wpływu stosowanych w budownictwie jednorodzinym ścian wykonanych z cegieł na wartości natężenia pola elektrycznego. Rozpatrywano trzy rodzaje cegieł, z których została wykonana ściana (cegła pełna, cegła z 18 drążeniami i cegła z 30 drążeniami). W analizie uwzględniono także wpływ rozmiaru drążenia na wartości pola oraz zmienność konduktywności cegły. Porównano wyniki dla układu z asymetrycznym rozłożeniem cegieł z układem symetrycznym, który może odpowiadać ścianom zbudowanym z pustaków. Analiza dotyczyła częstotliwości stosowanej w komunikacji bezprzewodowej (Wi-Fi), tj. $f=2,4$ GHz. Omówiono wpływ rozmiaru drążenia i konduktywności cegły na wartości pola elektrycznego. Do analizy zastosowano metodę opartą na równaniach Maxwella, czyli metodę różnic skończonych w dziedzinie czasu. (Analiza wpływu konduktywności cegieł, rodzaju cegieł i rozmiaru drążenia na wartości natężenia pola elektrycznego).

Keywords: electromagnetic waves propagation, finite difference time domain method (FDTD), wireless communication, building materials.
Słowa kluczowe: propagacja fal elektromagnetycznych, metoda różnic skończonych w dziedzinie czasu (FDTD), komunikacja bezprzewodowa, materiały budowlane.

Introduction

Wireless networks are a proven, modern solution used in the creation of telecommunications systems. Their use allows you to replace the cabling used in standard LAN (Local Area Network) or wide area networks (WAN). Wireless data transmission systems allow for relatively easy and quick connection of multiple devices, while maintaining the possibility of dynamic and automatic configuration of a set of communicating elements. Maintaining the proper quality of communication in the selected area, including the stability of the connections set up and the transmission speed, remains an essential issue when installing wireless communication systems. The discussed problems become particularly important when installing wireless networks inside buildings. The reason is the effects of the propagation of electromagnetic waves in systems with complex geometry and material structure.

The final configuration of wireless networks requires appropriate measurements and tests in real conditions. At the stage of designing and analysing the network structure, it is also possible to use computer modelling methods. Numerical analysis of the phenomena of electromagnetic wave propagation allows taking into account the structure of the building and performing a multi-variant analysis of the designed wireless communication system.

The issues presented in the publications take into account construction technologies to a limited extent, taking into account the internal structure of elements or the diversity of material properties (e.g. clinker bricks, reinforcement, hollow blocks). Single-family houses contain walls that consist mainly of various types of bricks. The location of wireless communication systems (Wi-Fi) inside such buildings requires the analysis of changes occurring during the propagation of an electromagnetic wave. In the available literature [1-7] it can be seen that most of the authors focus on the analysis of homogeneous building materials (e.g. concrete slabs or solid bricks). The propagation of EM waves in this type of materials is predictable and can be calculated using analytical methods.

It should be emphasized that the field distribution inside rooms is influenced not only by wave attenuation, but also by multiple reflections caused by the complex structure of the building material. Due to electromagnetic phenomena, the material from which the structure is made is of great importance. Due to the fact that it is becoming more and more common to charge everyday devices with the use of Wireless Power Transfer (WPT) technology [8], an important aspect is the construction of walls on which sources can be attached, such as in the case of charging lamps [9]. The influence of the dielectric, which is the wall, has a significant impact on the quality of data transmission [10].

The article presents an analysis of the EM field distribution in the area containing a wall made of three types of bricks. The analysis also took into account the variability of the conductivity of the brick. In their articles, the authors assumed different values of the electric parameters of bricks (permittivity $\epsilon_r=3.7\div 19$ [11], $\epsilon_r=4.62\div 4.11$ [12], or conductivity ($\sigma=0.00278\div 0.244$ S/m) [12-14].

In order to assess the effect of brick complexity (ceramic and hollow material) on the values of the electric field strength, the variants with different percentages of clay mass in the brick were analysed. The analysis of the electric field created as the result of EM wave propagation through a wall made of various types of bricks will let to understand the processes, which take place in environments with a non-homogenous dielectric.

Analysed models

In the macroscopic approach, reinforced concrete and hollow bricks are classified as complex building structures. Bricks are made of clay or other clay materials with the addition of sand, then dried and fired at high temperature. The division of finished products concerns geometrical features, compressive strength, degree of burnout and the raw materials used [3]. The dimensions of the bricks vary widely, but are based on the ratio of height (h) to width (b)

and length (l) of 1: 2: 4 (Figs. 1, 2). In complex structure like brick with hollows the distribution of the field may only be performed by usage of numerical analysis. In this article, the presented analysis is of three commonly used walls made of three types of building material:

- 1) solid brick (Fig. 1a);
- 2) brick with 18 vertical hollows (marked as B18) (Figs. 1b, 2b);
- 3) brick with 30 vertical hollows (B30) (Figs. 1c, 2c).

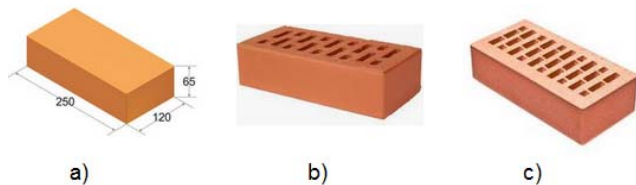


Fig.1. Models of analysed bricks: a) solid brick; b) B18; c) B30

The changeability of the width of the hollows (r_o) along the length of the brick (l) was analysed. The following sizes of hollows were analysed: $r_o \in \{0, 0.005, 0.007, 0.011, 0.013, 0.015, 0.017\}$ m}.

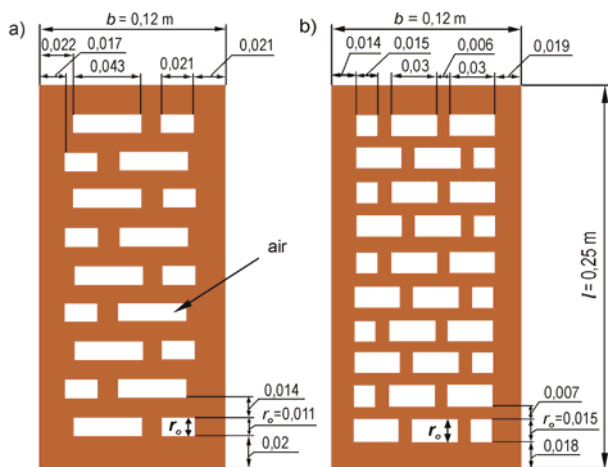


Fig.2. Geometrical sizes of two types of analysed brick: a) B18 and b) B30

The size of the hollow influences the percentage share of the loss dielectric (clay mass) in the brick (v) (Table 1). Red colour signifies the values of the typical hollow sizes in two types of hollow clay bricks. Bold type was used to signify the two closest v values in various sizes of hollows.

Table 1. The percentage of the clay inside the analysed bricks dependent on the size of hollows

Size of hollows inside the brick, changed along axis Ox	Relative volume of the clay in the brick (v) [%]	
r_o [m]	Brick (B18)	Brick (B30)
0.005	90.40	87.50
0.007	86.56	82.50
0.009	82.72	77.50
0.011	78.88	72.50
0.013	75.04	67.50
0.015	71.20	62.50
0.017	67.36	57.50

The analysis included the influence of brick arrangement (Fig. 3). It was verified whether the asymmetric system (Figs. 3a, 3c) greatly influences the field intensity values compared to the symmetrical system (Figs. 3b, 3d), which is the equivalent of hollow bricks.

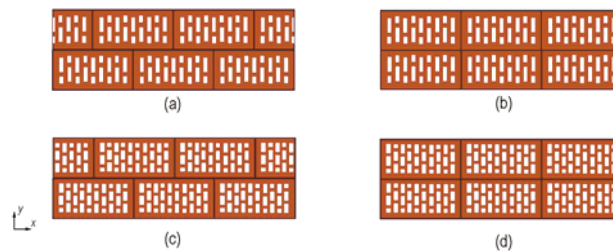


Fig.3. The four kinds of analysed wall: a) asymmetric composed of B18 bricks (B18_asym); b) symmetric composed of B18 bricks (B18_sym); c) asymmetric composed of B30 bricks (B30_asym); d) symmetric composed of B30 bricks (B30_sym)

The analysis concerned the frequency $f=2.4$ GHz for which the length of the EM wave propagating in air was $\lambda_p=0.125$ m. To analyse the researched variants, a relative electrical permittivity of $\epsilon_r=4.44$ was determined [11, 14], whereas the conductivity was modified within the range $\sigma=0 \div 0.2$ S/m.

Numerical model

To determine the distribution of the electromagnetic field, the finite difference time domain method (FDTD) was used [15]. This method is useful in the numerical analysis of high frequency time dependent electromagnetic fields.

The method is based on the transformations of Maxwell's equations into a differential form [15, 16]:

$$(1) \quad \nabla \times \mathbf{H} = \sigma \mathbf{E} + \epsilon \frac{\partial \mathbf{E}}{\partial t},$$

$$(2) \quad \nabla \times \mathbf{E} = -\mu \frac{\partial \mathbf{H}}{\partial t}.$$

The field distribution in the analysed domain is calculated by direct integration method in time and space. Hence, for instance, the equation describing E_z component in the Cartesian coordinate system is determined from the following dependence:

$$(3) \quad \frac{\partial E_z}{\partial t} = \frac{1}{\epsilon} \left(\frac{\partial H_y}{\partial x} - \frac{\partial H_x}{\partial y} - \sigma E_z \right).$$

As a result of the approximation of partial derivatives Maxwell's equation in a differential form is obtained. For this case equation (3) takes the shape of:

$$(4) \quad \frac{E_z|_{i,j,k}^{n+1} - E_z|_{i,j,k}^n}{\Delta t} = \frac{1}{\epsilon} \left(\frac{H_y|_{i+1/2,j,k}^{n+1/2} - H_y|_{i-1/2,j,k}^{n+1/2}}{\Delta x} - \frac{H_x|_{i,j+1/2,k}^{n+1/2} - H_x|_{i,j-1/2,k}^{n+1/2}}{\Delta y} - \sigma E_z|_{i,j,k}^{n+1/2} \right),$$

which, after transformation, allow us to determine the value of E_x component of the electric field intensity at observation point $(i, j+1/2, k+1/2)$ in time $(n+1/2)$ basing on the

components of the magnetic field in the previous moment t at suitable points of space.

The discretization in the space is performed by an appropriate location the vectors of both electric and magnetic field intensity within each cell. The vector components of the electromagnetic field are calculated for different points of space. The vector components of the electric field intensity assigned to Yee cell are placed in the middle of the respective edges whereas the components of the magnetic field intensity are placed in the middle points of the side walls.

The integration of Maxwell's equations in the time domain is based on the leap-frog scheme. The points of time at which the distribution of electric field vector \mathbf{E} is determined, are displaced by $\Delta t/2$ with respect to the points where the component values of magnetic field intensity vector \mathbf{H} is calculated. Every Yee cell is described by such material parameters, among others, as electric conductivity or magnetic permeability.

The stability of the time marching explicit scheme requires satisfying the Courant-Friedrichs-Lewy (CFL) condition [15-16]. This condition determines the relationship between time step in the leap-frog scheme of FDTD method and the maximum size of Yee cell [15]. The analysed area was composed of Yee cells (0.001 m).

The source of the field was a sinusoidal oscillating plane wave with $f=2.4$ GHz. The EM field is excited in a region far away of the wall. The absorption of the incident and reflected waves are obtained using perfectly matched layer boundary conditions (PML) [15-16]. These were entered perpendicular to the equiphase surface.

The purpose of this analysis was to analyse the field intensity in the area behind the four wall variants. The models assumed periodic boundary conditions (periodical Bloch boundary conditions were assumed at the edges perpendicular to the Ox axis) [15-16].

Results and discussion

Figures 4-11 show the distribution of E_z component behind the wall. The results of calculation are shown at the time when the steady state of the EM field distribution had been achieved.

Figures 4-7 shows the changes in the maximum relative value of the E_z component depending on the conductivity value of the brick material and the size of the hollows (r_o) for four type of the wall. Considerable loss of material causes the characteristics to run similar to variants with homogeneous lossy material. Increasing the size of the gaps (air area) at the expense of the lossy dielectric lowers the resultant wave attenuation. The characteristics for both C18 and C30 bricks are monotonic.

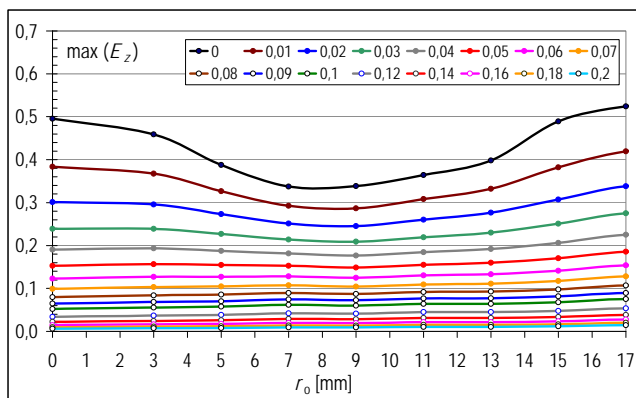


Fig.4. The relative maximum values of E_z component behind the wall made of B18 bricks (model asymmetric – B18_asy)

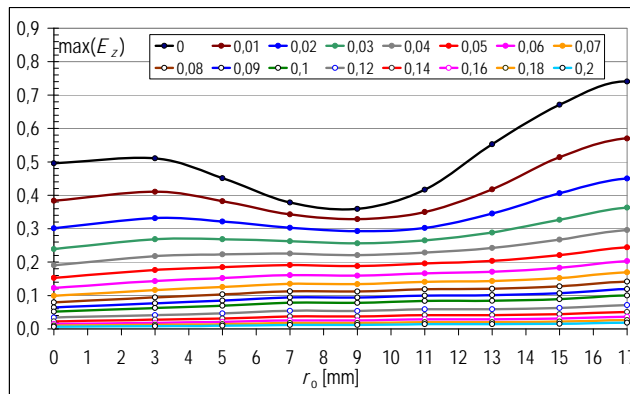


Fig.5. The relative $\max(E_z)$ component behind the wall made of B18 bricks (model symmetric – B18_sym)

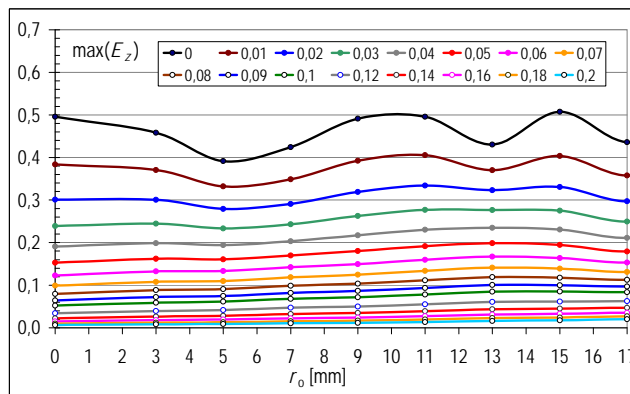


Fig.6. The relative maximum values of E_z component behind the wall made of B30 bricks (model asymmetric – B30_asy)

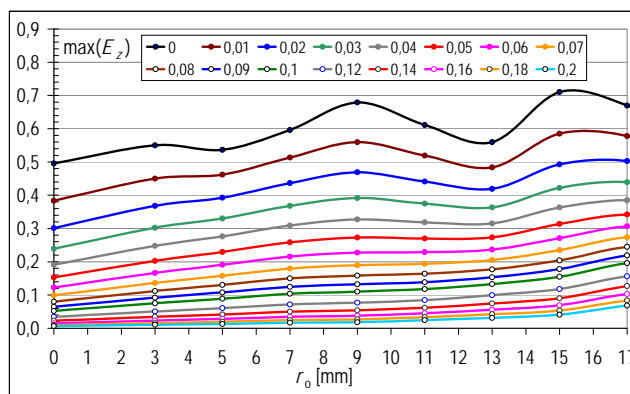


Fig.7. The relative $\max(E_z)$ component behind the wall made of B30 bricks (model symmetric – B30_sym)

Comparing the graphs showing the relationship between the size of the drill and the field intensity, it can be seen that the shape of the characteristics for symmetrical and asymmetrical models is similar for the same type of wall (C18 or C30) (Figs. 4-7). For the asymmetric wall made of C18 bricks, a significant reduction in the value of the electric field in the range $r_o \in \{0.005-0.013\}$ m (Fig. 4) can be noticed. For the symmetric model, the reduction in values is in a similar range, with the lowest values being for $r_o=8$ and $r_o=9$ (Figs. 4-5).

On the other hand, when analysing the characteristics for walls made of bricks with a greater number of hollows (B30_asy, B30_sym), the decrease in the value occurs in the range $r_o \in \{0.003-0.007\}$ m and for $r_o=13$ (Figs. 6-7). In the case of models with a greater number of hollows, the highest values are practically for $r_o=9$. In the models made of C18, the values were the lowest for this hollows size. In

all variations, along with the increase in conductivity, the field intensity values decrease (Figs. 4-7), which, of course, is in line with the laws of physics. It is important to emphasize that in symmetric models the E_z component values are even 40% higher than for the corresponding asymmetric models. On this basis, it can be concluded that the values of the area for walls made of structural clay tile will be higher than for walls made of two rows of bricks arranged with a shift of half a brick (asymmetric models).

On Figs. 8-11 the relationships between conductivity and electric field values are presented. Based on all the characteristics, it can be seen that with the increase in conductivity, the E_z component values decrease regardless of the type of brick (i.e. solid brick, C18, C30) and the number of hollows.

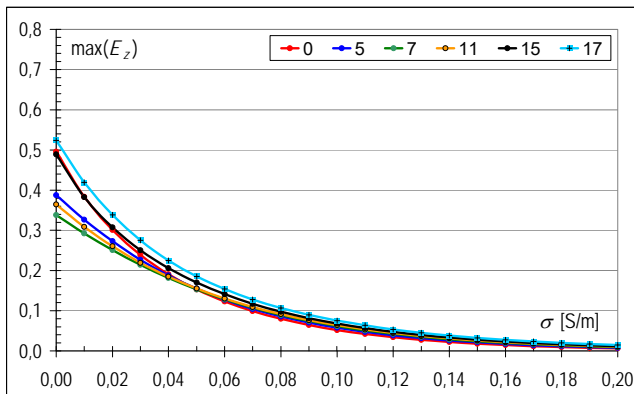


Fig.8. The relationship between conductivity and the size of hollow in the model B18_asym

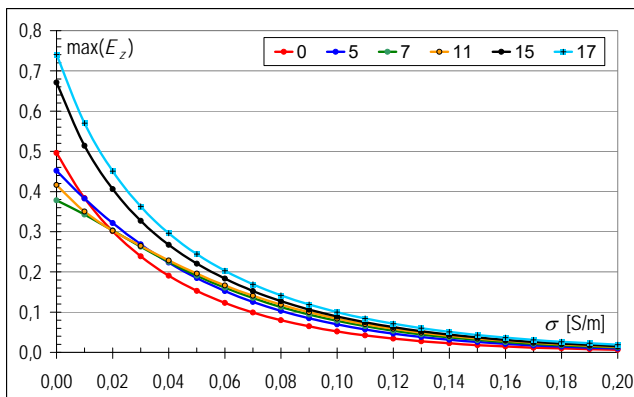


Fig.9. The relationship between conductivity and the size of hollow in the model B18_sym

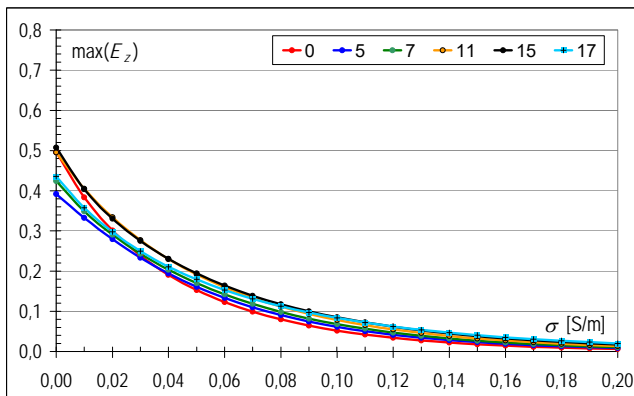


Fig.10. The relationship between conductivity and the size of hollow in the model B30_asym

When comparing the impact of the hollows size for asymmetric models, the differences in the field intensity

values are up to 5% in the range of $\sigma \in (0.05-0.2)$ S/m (Figs. 8, 10). On the other hand, for symmetrical models, greater probabilities in the field intensity are visible, and especially for the B30_sym model (Fig. 11). The results of the analysis of this model also show that in the entire conductivity range, the field values are higher for all hollows conditions than for a solid brick. This relationship is also visible in the case of a brick with a smaller number of hollows (C18_sym) but only in the range $\sigma \in (0.02-0.2)$ S/m (Fig. 9).

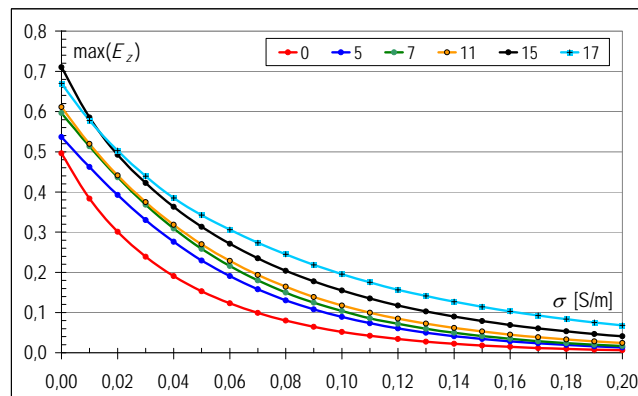


Fig.11. The relationship between conductivity and the size of hollow in the model B30_sym

Basing on the presented graphs, it may be claimed that the comparable v value (Table 1) does not influence achieving of the predicted maximum values of the E_z component. The reason for this are the multiple reflections and interference at the air-brick border.

Increasing the hollow area reduces the resultant damping of the entire brick area. When analysing lossless materials or materials with a relatively low loss $\sigma \in (0-0.1)$ S/m, the characteristics for C30 bricks have a more complex course than for C18 bricks. The local change in the speed of the electromagnetic wave as it passes through successive areas of bricks results in the formation of interference. Along with the reduction of the conductivity value, this effect is less rapid, because the course of the phenomena is mainly determined by the loss of the ceramic mass.

The results prove the complex wave phenomena occurring during wave propagation through a complex material. Various wall structures or the variability of material parameters require individual analysis.

Conclusions

The propagation of the EM wave in the area of the brick is a complex process. The structure of brick with hollows affects the occurrence of multiple reflections at the air-ceramic interface. The number and size of openings in the brick cause temporary changes in the field image in the area just behind the wall.

The obtained results indicate that the reduction of the percentage of ceramic mass in the brick leads to an increase in the absolute value of the field strength. This is the expected effect due to the reduction of the absolute layer thickness of the lossy dielectric. However, the observed changes in the field intensity significantly depend on the field effects, multiple reflections on the ceramic mass-air interface and the size of the drillings in relation to the electromagnetic wave length. These types of phenomena can be quantified through numerical calculations.

The differences in the field value are greater in the case of the B30 brick. The smaller number of hollows and their

widths result in less distortion of the EM wave. In the case of a wall where the attenuation is negligible ($\sigma < 0.01$ S/m) or equal to zero, the effects of wave attenuation play a much greater role.

This work was supported by the Ministry of Science and Higher Education in Poland at the Białystok University of Technology under research subsidy No. WZ/WE-IA/2/2020.

Author: dr inż. Agnieszka Choroszucho, Białystok University of Technology, Faculty of Electrical Engineering, Department of Electrical Engineering, Power Electronics and Power Engineering, Wiejska 45D, 15-351 Białystok,
E-mail: a.choroszucho@pb.edu.pl

REFERENCES

- [1] Yang M., Stavrou S., Rigorous coupled-wave analysis of radio wave propagation through periodic building structures, *IEEE Antennas and Wireless Propagation Letters*, Vol. 3 (2004), 204-207
- [2] Cuinas I., Sanchez M.G., Permittivity and conductivity measurements of building materials at 5.8 GHz and 41.5 GHz, *Wireless Personal Communications*, 20 (2002), 93-100
- [3] Stavrou S., Saunders S.R., Review of constitutive parameters of building material, *IEEE Transactions on Antennas and Propagation*, Vol. 1 (2003), 211-215
- [4] Antonini G., Orlandi A., D'elia S., Shielding effects of reinforced concrete structures to electromagnetic fields due to GSM and UMTS systems, *IEEE Transactions on Magnetic*, 39 (2003), No. 3, 1582-1585
- [5] Dalke R.A., Holloway Ch.L., McKenna P., Johannson M., Ali A.S., Effects of reinforced concrete structures on RF communications, *IEEE Transactions on Electromagnetic Compatibility*, 42 (2000), No. 4, 486-496
- [6] Liu Ping, Chen Gui, Long Yun-liang, Effects of reinforced concrete walls on transmission of EM wave in WLAN, *Proceedings of the ICMMT 2008, International Conference on Microwave and Millimeter Wave Technology*, Vol. 2 (2008), 519-522
- [7] Peña D., Feick R., Hristov H.D., Grote W., Measurement and modeling of propagation losses in brick and concrete walls for the 900 MHz band, *IEEE Transactions on Antennas and Propagation*, 51 (2003), No. 1, 31-39
- [8] Stankiewicz J.M., The analysis of the influence of the plane coils geometry configuration on the efficiency of WPT system, *Przeгляд Elektrotechniczny*, 96 (2020), no. 10, 174-178
- [9] Zhao M., Miyamoto T., Optimization for Compact and High Output LED-Based Optical Wireless Power Transmission System, *Photonics*, 9 (2022), 14, <https://doi.org/10.3390/photonics9010014>
- [10] Stankiewicz J.M., Comparison of the efficiency of the WPT system using circular or square planar coils, *Przeгляд Elektrotechniczny*, 97 (2021), no. 10, 38-43
- [11] Shah M.A., Hasted J.B., Moore L., Microwave absorption by water in building materials: aerated concrete, *British Journal of Applied Physics*, Vol. 16 (1965), No. 11, 1747-1754
- [12] Landron O., Feuerstein M.J., Rappaport T.S., A comparison of theoretical and empirical reflection coefficients for typical exterior wall surfaces in a mobile radio environment, *IEEE Transactions on Antennas and Propagation*, Vol. 44 (1996), No. 3, 341-351
- [13] Tan S.Y., Tan Y., Tan H.S., Multipath delay measurements and modeling for interfloor wireless communications, *IEEE Transactions on Vehicular Technology*, 49 (2000), No. 4, 1334-1341
- [14] Pinhasi Y., Yahalom A., Petnev S., Propagation of ultra wide-band signals in lossy dispersive media, *IEEE International Conference on Microwaves, Communications, Antennas and Electronic Systems, COMCAS* (2008), 1-10
- [15] Taflove A., Hagness S.C., Computational electrodynamics, The Finite-Difference Time-Domain Method. Boston, Artech House, (2005)
- [16] Oskooi A.F., Roundyb D., Ibanescua M., Bermelc P., Joannopoulousa J.D., Johnson S.G., MEEP: A flexible free-software package for electromagnetic simulations by the FDTD method, *Computer Physics Communications*, Vol. 181 (2010), 687-702